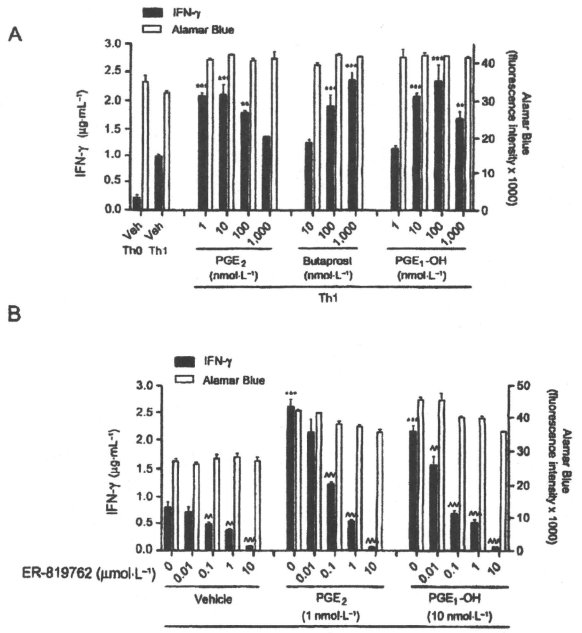

Figure 2 EP_4 receptor antagonism selectively suppresses prostaglandin E_2 (PGE_2)-induced Th1 differentiation *in vitro*. (A) Naive $CD4^+$ T cells from BALB/c mice were stimulated with α-CD3/α-CD28 under Th1-promoting conditions (see *Methods*) in media supplemented with 10% charcoal-stripped fetal bovine serum (FBS), together with PGE_2, butaprost, or PGE_1-OH at the indicated concentrations. After 3 days, interferon (IFN)-γ production was analysed by enzyme-linked immunosorbent assay (ELISA) and cell proliferation/viability was monitored by AlamarBlue. (B) was the same as (A), except that cells were cultured in the presence or absence of the indicated concentrations of PGE_2, PGE_1-OH and/or ER-819762. (C) Naive $CD4^+$ T cells isolated from DO11.10 mice were stimulated with ovalbumin (OVA)/antigen-presenting cells (APCs) under Th1-promoting conditions in 10% normal FBS in the presence or absence of ER-819762 and/or anti-PGE_2 for 3 days. IFN-γ production in culture supernatants was analysed by ELISA and cell proliferation/viability was monitored by AlamarBlue assay. (D) Naive $CD4^+$ T cells isolated from DO11.10 mice were stimulated with OVA/APCs under Th2-promoting conditions in normal 10% FBS in the presence or absence of ER-819762 for 6 days. Cells were collected at day 6 and re-stimulated with α-CD3 overnight. Cytokine [interleukin (IL)-4, left; IL-10, right] production in culture supernatants was analysed by ELISA. All data are shown as means ± SD ($n = 3$). Statistical analysis was performed by Dunnett-type multiple comparison test. *, ^ indicate $P < 0.05$; **, ^^ indicate $P < 0.01$ and ***, ^^^ indicate $P < 0.001$ levels of significance. *, **, *** induction compared with Th1, vehicle, no ER-819762 control. ^, ^^, ^^^ inhibition compared with untreated controls within each group. These data are representative of at least two independent experiments.

not charcoal-stripped FBS for this experiment. These results suggest that PGE_2 signalling via EP_4 receptors results in an increase in IL-17 production and/or in the fraction of IL-17-producing cells in the population while suppressing non-Th17 cell proliferation. These results also indicate that PGE_2 produced by the T cells themselves and/or present in serum is involved in IL-17 production or/and Th17 cell expansion. Stimulation of these cells in the presence of PGE_2 or PGE_1-OH enhanced expression of IL-23 receptors, the retinoic acid receptor-related orphan receptor γ-T and IL-17A mRNA (Supplementary Fig. 5A). PGE_2-induced up-regulation of IL-23 receptors and IL-17A mRNA was suppressed by ER-819762 or anti-PGE_2 antibodies (Supplementary Fig. 5B and data not shown). IL-17 production and the percentage of IL-17-producing cells were also increased by other cAMP-inducing agents including butaprost or forskolin (Fig. 5A and C), suggesting a possible role for cAMP signalling in this process. No significant enhancement of PGE_2 on Th17 cell differentiation was observed when naïve $CD4^+$ T cells were activated in the presence of transforming growth factor (TGF)-β + IL-6, and no inhibitory effect of ER-819762 was observed in this system (data not shown).

EP_4 receptor antagonist suppresses inflammatory arthritis

As Th1 and Th17 cells have been implicated in the pathogenesis of autoimmune diseases such as RA (Schulze-Koops and

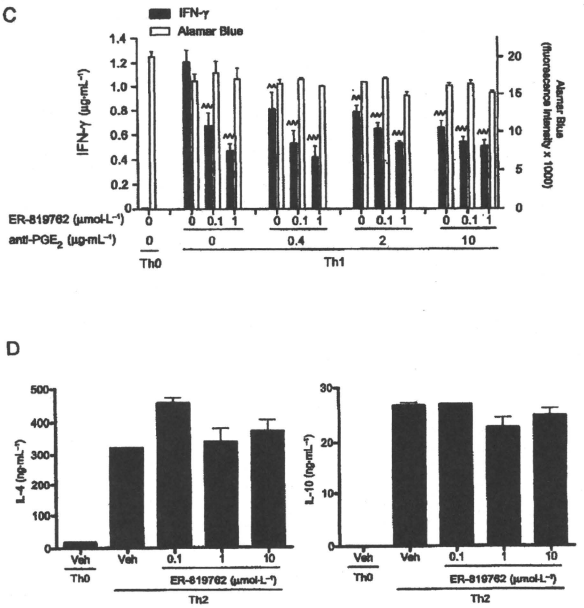

Figure 2 *Continued.*

Kalden, 2001; Fouser *et al.*, 2008), we tested whether the selective EP_4 receptor antagonist ER-819762 might influence disease in two mouse models of RA. We first tested the effect of ER-819762 in the murine CIA model, an animal model widely used for assessing therapeutic agents for treatment of RA. When given orally prior to the onset of disease, ER-819762 dose-dependently suppressed the clinical signs of arthritis and delayed disease onset (Fig. 6A). ER-819762 also significantly suppressed disease progression when it was administered subsequent to the onset of disease (Fig. 6B). Furthermore, ER-819762 retarded bone erosion in the CIA model, as demonstrated by radiological evaluation (Fig. 6C).

Matsumoto *et al.* (2008) have suggested that the GPI-induced arthritis model is more predictive of clinical efficacy than the CIA model, as the therapeutic effects of anti-tumour necrosis factor (TNF), anti-IL-6 and CTLA-4/Ig fusion in the GPI-induced arthritis model are similar to those seen in human patients treated with the equivalent biological agents. In the GPI-induced arthritis model in DBA/1 mice, oral administration of ER-819762 significantly reduced arthritis severity and delayed disease onset when administered prior to the onset of disease (Fig. 7A). ER-819762 also significantly suppressed disease progression when administered after the establishment of arthritis (Fig. 7B). Collectively, these results demonstrate that ER-819762 not only prevents the development of inflammatory arthritis, but is effective against the established disease by reducing both inflammation and joint destruction in animal models of RA.

Suppression of Th1 and Th17 responses in vivo

To determine whether suppression of arthritis by ER-819762 is associated with reduced Th1 and Th17 responses, we performed *ex vivo* challenge of cells obtained from mice with CIA. Cultured lymph node cells obtained from CIA mice were challenged *ex vivo* with collagen and cytokine production was determined. Cells from mice that had been treated with ER-819762 had significantly lower production of IFN-γ (>90%), IL-17 (>80%), TNF-α (>60%), IL-6 (>70%), osteopontin (>55%) and the chemokine CCL3 (MIP-1α; >35%) compared with lymph node cells from vehicle-treated mice (Fig. 6D). Overall lymph node cell proliferation was suppressed in ER-819762-treated mice to levels similar to those in non-immunized mice (data not shown).

We next examined the frequency of Th1 and Th17 cells found in the lymph nodes of GPI-induced arthritic mice. Popliteal lymph nodes were obtained from naïve, vehicle- or ER-819762-treated animals at 6 days post immunization and analysed by intracellular IFN-γ and IL-17 staining. The percentage of IL-17- and IFN-γ-producing $CD4^+$ T cells was

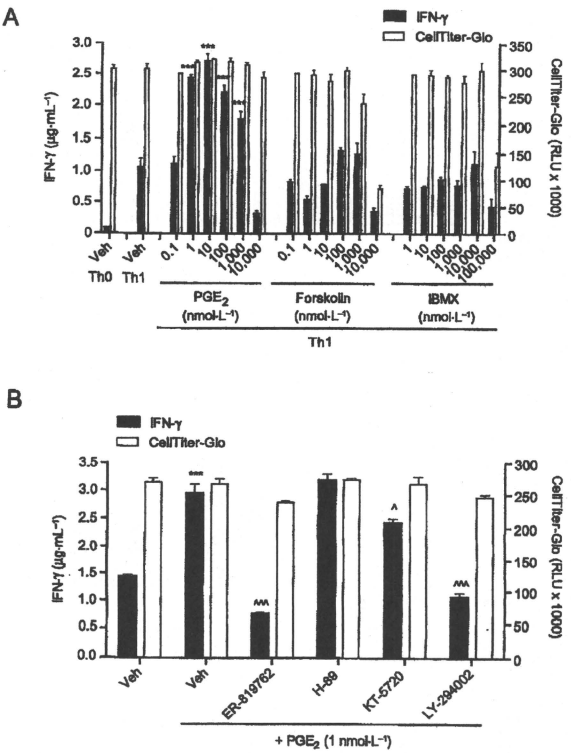

Figure 3 Enhancement of Th1 differentiation by EP_4 receptor stimulation requires phosphatidylinositol 3-kinase (PI3K) signalling. (A) The effect of cyclic AMP-inducing agents on Th1 differentiation was examined using the same methods as in Figure 2A. Cell proliferation/viability was monitored with CellTiter-Glo. (B) The effect of PKA and PI3K inhibitors on Th1 differentiation was examined as in (A). Inhibitor concentrations were as follows: 1 μmol·L^{-1} H-89, 10 μmol·L^{-1} KT-5720, 2 μmol·L^{-1} LY-294002 and 1 μmol·L^{-1} ER-819762. All data are shown as means ± SD ($n = 3$). Statistical analysis was performed by Dunnett-type multiple comparison test. *, ^ indicate $P < 0.05$; **, ^^ indicate $P < 0.01$ and ***, ^^^ indicate $P < 0.001$ levels of significance. *, **, *** induction compared with Th1, vehicle, no ER-819762 control. ^, ^^, ^^^ inhibition compared with untreated controls within each group. These data are representative of at least two independent experiments.

significantly lower in ER-819762-treated mice compared with vehicle-treated controls (Fig. 7C). The serum levels of IL-17 and IFN-γ were also significantly decreased in ER-819762-treated animals (Fig. 7D). Collectively these results indicate that EP_4 receptor-mediated PGE_2 signalling is important *in vivo* for the Th1/Th17 response and the development of inflammatory arthritis.

Suppression of CFA-induced hyperalgesia in rat

PGE_2 has been reported to be a key mediator of peripheral inflammatory pain, and evidence from studies using EP_4 receptor specific antagonists and small inhibitory RNAs implicate EP_4 receptors in this process (Lin *et al.*, 2006; Nakao *et al.*, 2007; Clark *et al.*, 2008). We therefore examined if ER-819762 might modulate the inflammatory pain response in a CFA-induced chronic inflammatory pain model in the rat. In this model, rats develop a lame walk reaction, characterized by a three-legged gait, 3 days after CFA injection. In the vehicle control group, 7 of 7 rats exhibited a positive lame walk reaction, while in the group treated with 100 mg·kg^{-1} ER-819762, 0 of 7 rats exhibited a positive lame walk reaction (Fig. 8). As a positive control, rats were also treated with the cyclooxygenase (COX) inhibitor, indomethacin and we observed significant suppression of lame walking at doses of 1 and 3 mg·kg^{-1} (Fig. 8).

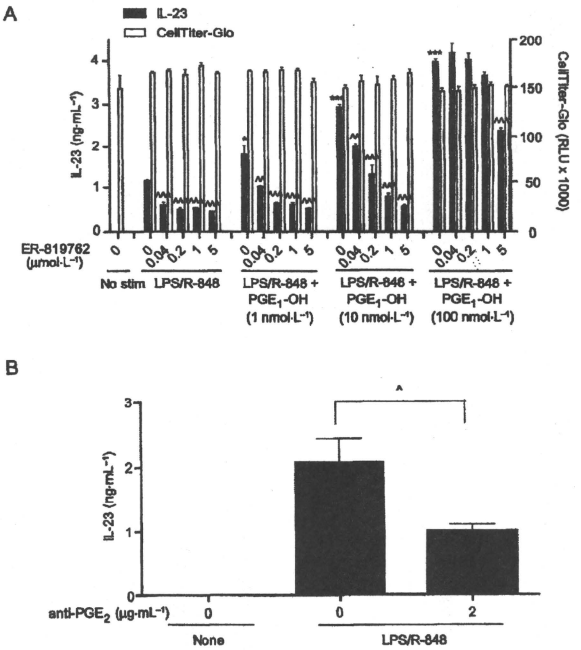

Figure 4 EP_4 receptor antagonism suppresses prostaglandin E_2 (PGE_2)-induced interleukin (IL)-23 production in human dendritic cells (DCs). (A) Human immature DCs were stimulated with 10 ng mL^{-1} lipopolysaccharide (LPS) and 2.5 μg mL^{-1} R-848 in the presence or absence of the indicated concentrations of PGE_1-OH and/or ER-819762 for 24 h. IL-23 in culture supernatants was measured by enzyme-linked immunosorbent assay and cell proliferation/viability was monitored with CellTiter-Glo. (B) Same as (A) but in the presence or absence of 2 μg mL^{-1} anti-PGE_2 antibody. All data are shown in means ± SD ($n = 3$). Statistical analysis was performed by Dunnett-type multiple comparison test: *, ^ indicate $P < 0.05$; **, ^^ indicate $P < 0.01$ and ***, ^^^ indicate $P < 0.001$ levels of significance. *, **, *** induction compared with LPS/R-848-stimulated, no-PGE_1-OH, no-ER-819762 control, ^, ^^, ^^^ inhibition compared with no-ER-819762 controls within each group. These data are representative of at least two independent experiments.

Discussion

In the present study, we describe the pharmacological actions of a novel and highly selective antagonist of the EP_4 receptor, ER-819762, in models of inflammation. We show that antagonism of EP_4 receptor activation can suppress Th1 differentiation, production of IL-23 in DCs, and Th17 cell expansion *in vitro*. In addition, when tested in two mouse models of RA, ER-819762 was very effective in suppressing disease symptoms *in vivo*. A significant body of research has linked Th1 and Th17 cell development and function to autoimmune disease (Schulze-Koops and Kalden, 2001; Fouser *et al.*, 2008), and we observe in the mouse RA disease models (CIA and G6PI) that treatment with ER-819762 suppresses the ability of lymph node T cells to produce IFN-γ and IL-17 *ex vivo* in response to stimulation. We also observed reduced levels of IFN-γ and IL-17 in the serum of ER-819762-treated versus control mice in the G6PI model (Fig. 7D). However, although the suppressive effects of ER-819762 observed *in vitro* and *in vivo* are consistent, we cannot directly attribute suppression of disease in the animal models to inhibition of Th1 or Th17 development or function *in vivo*. It is possible that suppression of EP_4 receptor signalling has other unknown pharmacological effects in these models. Nevertheless, these *in vitro* and *in vivo* results show that antagonism of EP_4 receptors can suppress a broad range of pro-inflammatory responses relevant to the development of autoimmunity.

These results were initially unexpected, as earlier studies had demonstrated that PGE_2 suppresses T cell-mediated inflammation by increasing intracellular cAMP, inhibiting Th1 cytokine IFN-γ production, and inhibiting T cell activation and proliferation (Betz and Fox, 1991; Gold *et al.*, 1994; Hilkens *et al.*, 1995; Okano *et al.*, 2006). However, more recent reports have demonstrated the pro-inflammatory effects of

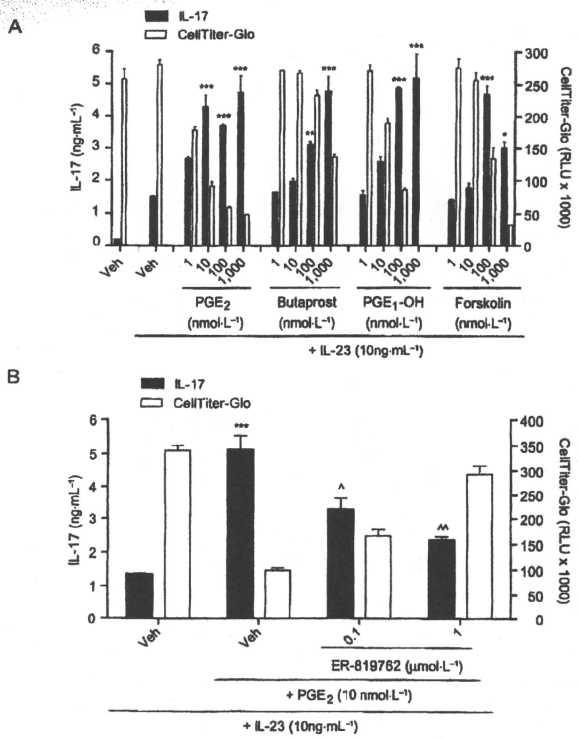

Figure 5 Prostaglandin E_2 (PGE_2)-EP_4 receptor signalling regulates Th17 cell development. (A) Total $CD4^+$ T cells isolated from mouse splenocytes were stimulated with anti-CD3/anti-CD28 plus interleukin (IL)-23 in the presence or absence of exogenous PGE_2, butaprost, PGE_1-OH, or forskolin for 3 days. IL-17 in culture supernatants was measured by enzyme-linked immunosorbent assay. (B) Same methods as in (A), except that ER-819762 was added at the indicated concentrations. (C) Total $CD4^+$ T cells were stimulated with α-TCRβ/α-CD28 ± IL-23 in the presence or absence of exogenously added PGE_2, butaprost, PGE_1-OH, or forskolin for 5 days and the percentage of Th17 cells was analysed by IL-17 intracellular staining. The horizontal broken line represents the level of IL-17 positive cells in the presence of IL-23 only. (D) Same methods as in (C), except that no PGs were added, and ER-819762 was added at the indicated concentrations. The number of Th17 cells was analysed by IL-17 intracellular staining. Upper plots show staining with control isotype-matched staining antibody, bottom plots show staining with anti-IL-17 antibody. First two columns show unstimulated and IL-23-stimulated cells. Right-hand lower two plots show IL-23-stimulated cells treated with different concentrations of ER-819762. All data are shown in means ± SD ($n = 3$). Statistical analysis was performed by Dunnett-type multiple comparison test: *, ^ indicate $P < 0.05$; **, ^^ indicate $P < 0.01$ and ***, ^^^ indicate $P < 0.001$ levels of significance. *, **, *** induction compared with lipopolysaccharide/R-848-stimulated, no-PGE_1-OH, no-ER-819762 control, ^, ^^, ^^^ inhibition compared with no-ER-819762 controls within each group. These data are representative of at least two independent experiments.

PGE_2 in Th17 development (Chizzolini *et al.*, 2008; Boniface *et al.*, 2009; Napolitani *et al.*, 2009) and DC activation (Sheibanie *et al.*, 2004; Khayrullina *et al.*, 2008). As antagonism of EP_4 receptor signalling suppressed Th1 differentiation, Th17 cell expansion, and the development of pathologies in mouse CIA- and GPI-induced arthritis, we propose that the immune stimulatory activities of PGE_2 are relevant to these diseases.

Another debilitating aspect of RA is the pain associated with joint inflammation. This inflammatory pain is mediated, at least in part, by PGE_2 stimulation of EP_4 receptors (Lin *et al.*, 2006; Nakao *et al.*, 2007). Selective inhibition of EP_4 receptor signalling by several different EP_4 receptor antagonists has been shown to cause a marked reduction in joint pain, mechanical and thermal hyperalgesia and oedema in rat and in guinea pig models of pain and inflammation, often with similar efficacy to that observed with selective COX-2 inhibitors such as rofecoxib (Lin *et al.*, 2006; Nakao *et al.*, 2007; Clark *et al.*, 2008; Murase *et al.*, 2008; Jones *et al.*, 2009). Consistent with these findings, we observed that ER-819762 was

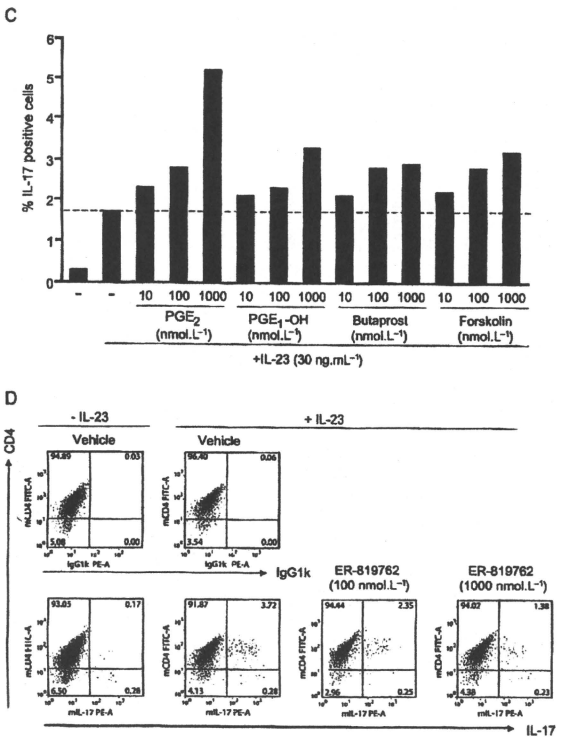

Figure 5 *Continued.*

effective in relieving inflammatory pain in a rat model of inflammatory pain induced by CFA injection into the paws. The analgesic effect of ER-819762 could be associated with reduced peripheral sensitization by suppression of PGE_2-mediated action on the peripheral terminals of nociceptor sensory neurons (Lin *et al.*, 2006). Alternatively, inhibition of IFN-γ and TNF-α by ER-819762 can also have an analgesic effect, because these cytokines have been shown to induce hypernociception (Verri *et al.*, 2006). Thus, an EP_4 receptor antagonist may have multiple benefits in relieving both the symptoms and modifying the disease mechanisms leading to RA.

EP_4 receptors have been reported to signal by at least two pathways (Regan, 2003): (i) activation of adenylate cyclase via the G_s protein to increase cAMP, and (ii) activation of PI3K via a G protein-independent signalling process. The suppression of T-cell activation by PGE_2 and other cAMP-elevating agents was proposed to be mediated by the activation of PKA, activation of C-terminal src kinase (Csk) and repression of leukocyte-specific protein tyrosine kinase (Lck)-dependent signalling through the T cell receptor (Mustelin and Tasken, 2003; Chemnitz *et al.*, 2006). In this study, however, we show that PGE_2 utilizes the PI3K pathway to promote Th1 differentiation (Fig. 3). Our data also suggest that the cAMP signalling pathway may promote Th17 expansion (Fig. 5), although our results are not definitive.

Recently, Chizzolini *et al.* (2008), Boniface *et al.* (2009) and Napolitani *et al.* (2009) have reported that PGE_2 can enhance the expansion and/or production of Th17 cells via cAMP signalling, and that this is accompanied by enhanced expression of IL-23R, IL-1R1, RORγt, the chemokine CCL20 and its receptor CCR6. Boniface *et al.* (2009) suggested that EP_2 receptors may be more important than EP_4 receptors for Th17 cell development and/or expansion, at least in human cells. We also observed enhanced IL-17 production and modest expansion of Th17 cells by incubation with the EP_2 receptor-selective agonist butaprost, but our data show that antagonism of EP_4 receptors is sufficient to suppress

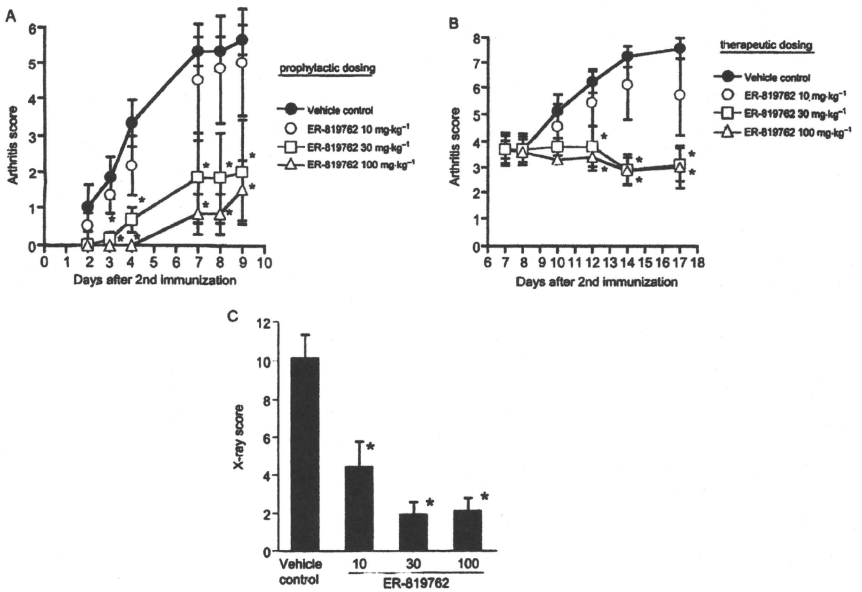

Figure 6 EP_4 receptor antagonism suppresses disease and Th1/Th17 cytokines in collagen-induced arthritis in mice. (A) DBA/1 mice were immunized with bovine type II collagen (bCII)/complete Freund's adjuvant (CFA) (primary immunization) and boosted with bCII in incomplete Freund's adjuvant at day 21 (second immunization) to induce arthritis as described in *Methods*. ER-819762 was orally administered daily from day 20 after primary immunization but before the onset of disease, and arthritis scores were monitored over the course of the study as described in *Methods*. (B) Same methods as in (A), but ER-819762 was administered after induction of disease on day 7 after second immunization. (C) Radiological analysis of inflamed paws at the end of the therapeutic collagen-induced arthritis study shown in 6B. The X-ray score is defined in *Methods*. (D) *Ex vivo* cytokine analysis. Mice were immunized with bCII/CFA or vehicle, similar to (A), except that ER-819762 was administered from the day of primary immunization (day 0). Lymph node cells were purified at day 15 and cultured in the presence of bCII (50 μg mL^{-1}) or phosphate-buffered saline for 72 h, and cytokine production was analysed. Statistical analysis was performed by Dunnett-type multiple comparison test compared with vehicle control (A–C) or paired *t*-test (D). Levels of significance: $^*P < 0.05$; $^{**}P < 0.01$; $^{***}P < 0.001$. These data are representative of at least two independent experiments.

PGE_2-mediated Th17 expansion and IL-17 production in mouse cells. Our data also showed that PGE_2 did not promote Th17 differentiation *per se*, as we did not see an increase in Th17 cell frequency following PGE_2 stimulation of purified naïve $CD4^+$ T cells in the presence of TGF-β and IL-6. Rather, we observed an increase in Th17 cells when total $CD4^+$ T cells were stimulated with PGE_2 in the presence of IL-23, indicating the expansion of pre-differentiated Th17 cells. Napolitani *et al.* (2009) suggested that PGE_2 acts by inhibiting expansion of $CCR6^-$ T cells rather than increasing the proliferation of $CCR6^+$ Th17 cells, independent of IL-23. In agreement with this report, we also observed enhanced IL-17 production by PGE_2 in the absence of IL-23 co-stimulation (data not shown). In addition, we showed that EP_4 receptor stimulation can enhance IL-23 production by activated human DCs and that this activity can be inhibited by a selective EP_4 receptor antagonist or anti-PGE_2 antibody in the presence or absence of exogenously added PGE_2. Sheibanie *et al.* (2007a) have also recently reported that PGE_2 exacerbates disease in the CIA mouse by enhancing DC IL-6 and IL-23 production, the latter of which maintains Th17 cell survival and proliferation and consequently promotes IL-17 production. Collectively, these results support the idea that PGE_2 stimulation of EP_4 receptors promotes Th17 cell expansion at two stages by: (i) enhancing IL-23 production by DCs, and (ii) directly acting on memory T cells to promote IL-17 production and Th17 cell expansion (Sheibanie *et al.*, 2004; Chizzolini *et al.*, 2008; Khayrullina *et al.*, 2008; Boniface *et al.*, 2009).

We observed that while low concentrations of PGE_2 promoted IFN-γ production under Th1-differentiation conditions, production started to decrease at higher concentrations of PGE_2 or PGE_1-OH without loss of cell viability (Figs 2A and 3A). Similar results were seen with higher concentrations of butaprost (data not shown). Thus, PGE_2 appears to have a bimodal effect on immune stimulation; promoting inflammation at lower concentrations while attenuating inflammation

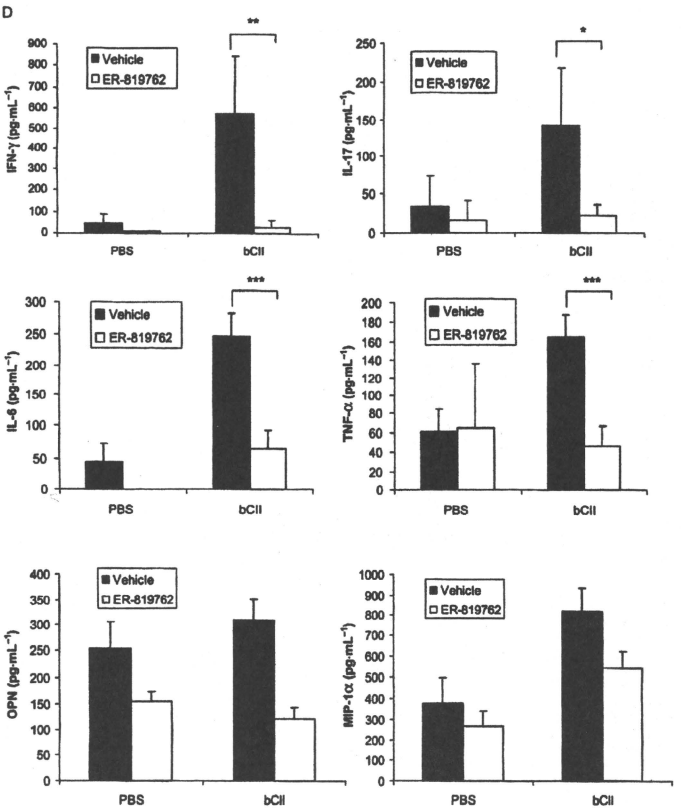

Figure 6 *Continued.*

at higher concentrations, possibly in concert with other factors that contribute to PI3K and/or cAMP signalling. This bimodal action may explain why PGE_2 exerts a pro-inflammatory effect in some systems and anti-inflammatory in others. For example, Betz and Fox (1991) have reported that PGE_2 can inhibit the production of Th1 cytokines, which is contrary to our results; however, these researchers used micromolar concentrations of PGE_2 for many of their experiments. There are also a number of potential sources of PGE_2 in cell culture systems that could contribute to higher PGE_2 levels. For example, our data suggest that autocrine production of PGE_2 can significantly contribute to Th1 differentiation, Th17 expansion and IL-23 production by DCs. We also observed that normal FBS, but not charcoal-stripped or PGE_2-immunodepleted serum stimulated EP_4 receptors in HEK/293 cells (Supplementary Fig. 1). Thus, there may be significant basal stimulation of EP_2 and EP_4 receptors in many cell culture systems, in which case further addition of exogenous PGE_2 could reduce inflammation.

COX inhibitors have also shown some efficacy in animal models of RA (Ochi *et al.*, 2003). Our results suggest that among the downstream effectors of the COX pathway, EP_4 receptors may play a particularly important role in the pathology of RA. In our own experiments, we saw only limited efficacy of the COX inhibitor indomethacin in suppressing arthritis in the mouse CIA model, and higher dosing was limited by toxicity (data not shown). Thus, a selective antagonist(s) of one or more critical downstream prostaglandin receptors may be more effective than broad inhibition of COX activity. Prostaglandins play a variety of

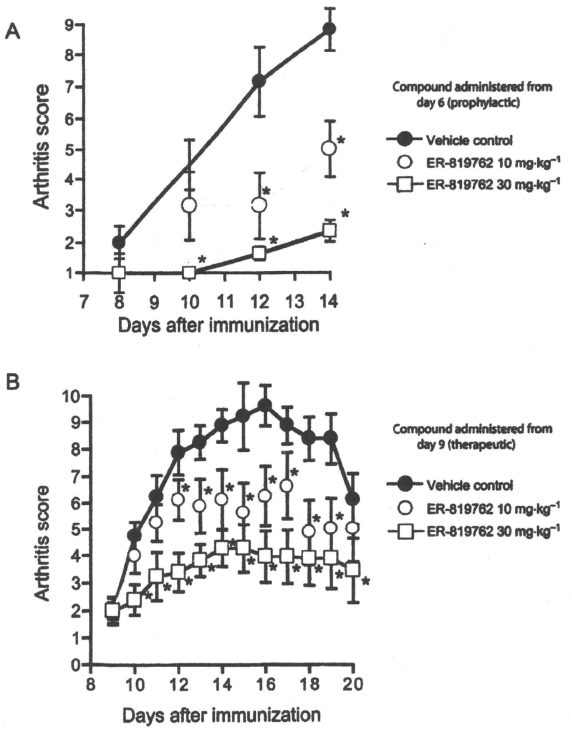

Figure 7 EP_4 receptor antagonism suppresses disease and Th1/Th17 cytokines in glucose-6-phosphate isomerase (GPI)-induced arthritis in mice. (A) DBA/1 mice were immunized with GPI/complete Freund's adjuvant to induce arthritis as described in *Methods*. ER-819762 was orally administered daily from day 6 after immunization, but before the onset of disease. Clinical scores were monitored over the course of the study. (B) Same methods as in (A), but ER-819762 was administered after disease induction (day 9). (C) Same methods as in (A), but ER-819762 was administered from the day of immunization. Popliteal lymph node cells were removed from mice at day 6 and re-stimulated with GPI in culture. Interleukin (IL)-17- and interferon (IFN)-γ-producing cells were quantified by intracellular staining and flow cytometry. Experiments with isotype control IgG are shown as cIgG. (D) Serum was collected at the end of the GPI study shown in (A), and analysed by IL-17 and IFN-γ enzyme-linked immunosorbent assay. Statistical analysis was performed by Dunnett-type multiple comparison test compared with vehicle control (A and B) or paired *t*-test (C and D). Levels of significance: $^*P < 0.05$; $^{**}P < 0.01$; $^{***}P < 0.001$. These data are representative of at least two independent experiments.

roles in modulating inflammation and can exert both anti- and pro-inflammatory effects. For example, one proposed explanation for why aspirin and other COX inhibitors are ineffective in treating allergic inflammation is that PGD_2 produced downstream of the COX enzymes stimulates the DP receptor, which promotes allergic inflammation, while PGE_2 stimulates the EP_3 receptor, which suppresses allergic inflammation (Kunikata *et al.*, 2005). In addition, the more targeted approach of antagonizing EP_4 receptors might suppress inflammation without the side-effects associated with some non-steroidal anti-inflammatory drugs and COX inhibitors, including increased gastrointestinal and cardiovascular risks. Consistent with this, Takeuchi *et al.* (2007) showed that the EP_4 receptor antagonist CJ-042794 did not produce any damaging effects in the gastrointestinal mucosa of control or adjuvant-induced arthritic rats, whereas indomethacin caused gross lesions. More importantly, we found that ER-819762 not only could prevent, but could suppress established disease in the CIA and GPI-induced arthritis models. Bone destruction in CIA was also significantly reduced by ER-819762. The effects of ER-819762 in suppressing bone destruction may be due in part to suppression of osteoclastogenesis promoted by IL-17 and PGE_2. IL-17 stimulates osteoblasts to synthesize PGE_2

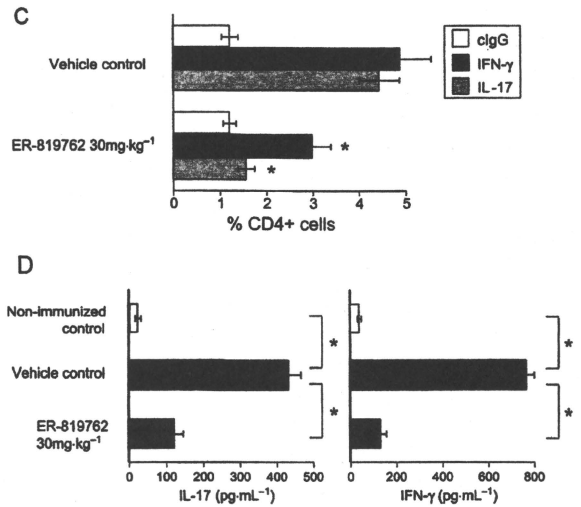

Figure 7 *Continued.*

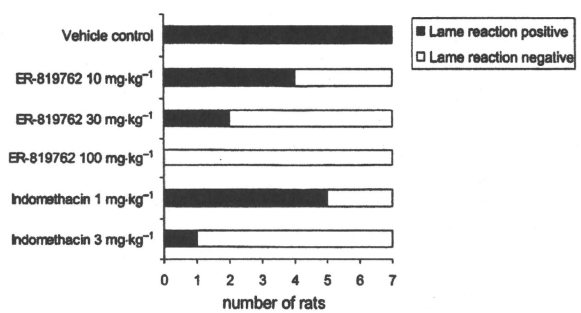

Figure 8 The analgesic effect of ER-819762 on the lame walk response in complete Freund's adjuvant (CFA) injected rats. CFA was injected into the right hind footpad of each rat (seven rats per treatment group). Three days after CFA injection, the rats exhibited a lame walking reaction as described in *Methods*. Compounds were given orally 3 days after CFA and the lame reaction was evaluated at 3 h after drug administration. These data are representative of at least two independent experiments.

and express receptor activator of NF-κB (RANK), which induces osteoclastogenesis (Kuligowska and Odrowaz-Sypniewska, 2004). We have observed that RANK-ligand mRNA levels in arthritic joints were lower in mice treated with an ER-819762 analogue in both the CIA and GPI-induced arthritis mouse models (unpublished results). Previous studies have also reported that anti-TNF-α therapy was effective in the GPI-induced arthritis model (Matsumoto *et al.*, 2008), but had little effect treating disease in the CIA model (Joosten *et al.*, 1996; Williams *et al.*, 2000). In contrast, ER-819762 was effective in both models, suggesting that an EP_4 receptor antagonist strategy may be beneficial to RA patients, including those who are insensitive to anti-TNF therapy.

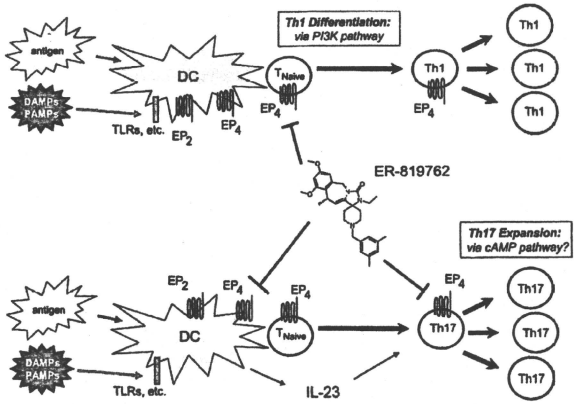

Figure 9 Multiple effects of ER-819762 on pro-inflammatory responses. Blue lines indicate the multiple steps at which ER-819762 was observed to exert an immunosuppressive effect in our studies. During infection or under conditions of chronic autoimmune inflammation, exogenous pathogen-associated molecular pattern stimuli (PAMPs) and/or endogenous danger-associated molecular pattern stimuli (DAMPs) drive immune cell activation in conjunction with antigen. In the case of Toll-like receptors, this signalling synergizes with the prostaglandin E_2 (PGE_2)-activated EP_4 receptor signalling pathway to enhance IL-23 production by dendritic cells (DCs). EP_4 receptor signalling in naïve T cells promotes their differentiation into Th1 effector cells via the phosphatidylinositol 3-kinase (PI3K) pathway, whereas EP_4 receptor signalling promotes the expansion of Th17 effector cells via the cyclic AMP pathway. ER-819762 blocks EP_4 receptor-enhanced Th1 differentiation and suppresses Th17 function both indirectly, by reducing DC IL-23 production and, as a consequence, Th17 survival, and directly by suppressing EP_4 receptor-enhanced Th17 expansion and/or IL-17 production. However, it is unknown if these actions of the EP_4 receptor antagonist can completely account for suppression of disease in the animal models, and other mechanisms are possible in addition.

These results and methodologies have been shared earlier with colleagues in another laboratory, and they have recently confirmed that PGE_2-EP_4 receptor signalling promotes Th1 cell differentiation, IL-23 production by DCs and Th17 cell expansion (Yao *et al.*, 2009). This group also tested an EP_4 receptor antagonist with a very different molecular structure from ER-819762, supporting the idea that the anti-inflammatory effects of ER-819762 are indeed due to EP_4 receptor antagonism and not due to action on another, unidentified target of the compound.

In summary, we show that an antagonist of EP_4 receptors, ER-819762, can suppress inflammation at multiple stages, as summarized in Fig. 9, as well as moderating inflammatory pain. Our results suggest that selective antagonism of EP_4 receptors could have therapeutic benefit in modifying both the underlying pathology of RA and alleviating pain, thus providing potential total management for RA patients.

Acknowledgements

We thank Tohru Arai (Eisai, Japan) for the HEK/293 cell line containing the CREB reporter, and Jesse Chow, Brian Gallagher, Icharu Hishinuma, Sally Ishizaka, Tim Chamberlain, Minlung Wang, Stephan Perron, Andrew Bender, Jeffrey Rose, Joanne Marsh, Kara Loiacono, Natalie Twine, Donna Young, Jane Daun, Frank Fang, and Jia Liu of Eisai Research Institute of Boston for important contributions to the experiments and discussion. We would like to particularly thank Professor Shuh Narumiya (Kyoto University), who was instrumental in providing confirmation of our early confidential results. The results in this manuscript were previously disclosed in PCT patent application publication WO 2009/064431 filed on 13 November 2008.

Conflict of Interest

All authors were employed by Eisai Inc. (USA) or Eisai Co., Ltd. (Japan) at the time of these studies. The authors have no further conflicting financial interests.

References

Alexander SPH, Mathie A, Peters JA (2009). Guide to Receptors and Channels (GRAC), 4th edn. *Br J Pharmacol* 158 (Suppl. 1): S1–S254.

Betz M, Fox BS (1991). Prostaglandin E2 inhibits production of Th1 lymphokines but not of Th2 lymphokines. *J Immunol* 146: 108–113.

Boniface K, Bak-Jensen KS, Li Y, Blumenschein WM, McGeachy MJ, McClanahan TK *et al.* (2009). Prostaglandin E2 regulates Th17 cell differentiation and function through cyclic AMP and EP2/EP4 receptor signaling. *J Exp Med* 206: 533–548.

Chemnitz JM, Driesen J, Classen S, Riley JL, Debey S, Beyer M *et al.* (2006). Prostaglandin E_2 impairs CD4$^+$ T cell activation by inhibition of lck: implications in Hodgkin's lymphoma. *Cancer Res* 66: 1114–1122.

Chizzolini C, Chicheportiche R, Alvarez M, de Rham C, Roux-Lombard P, Ferrari-Lacraz S *et al.* (2008). Prostaglandin E2

synergistically with interleukin-23 favors human Th17 expansion. *Blood* 112: 3696–3703.

Clark P, Rowland SE, Denis D, Mathieu MC, Stocco R *et al.* (2008). MF498, a selective E prostaglandin receptor 4 antagonist, relieves joint inflammation and pain in rodent models of rheumatoid and osteoarthritis. *J Pharmacol Exp Ther* 325: 425–434.

Fouser LA, Wright JF, Dunussi-Joannopoulos K, Collins M (2008). Th17 cytokines and their emerging roles in inflammation and autoimmunity. *Immunol Rev* 226: 87–102.

Fujino H, Xu W, Regan JW (2003). Prostaglandin E2 induced functional expression of early growth response factor-1 by EP4, but not EP2, prostanoid receptors via the phosphatidylinositol 3-kinase and extracellular signal-regulated kinases. *J Biol Chem* 278: 12151–12156.

Gold KN, Weyand CM, Goronzy JJ (1994). Modulation of helper T cell function by prostaglandins. *Arthritis Rheum* 37: 925–933.

Hata AN, Breyer RM (2004). Pharmacology and signalling of prostaglandin receptors: multiple roles in inflammation and immune modulation. *Pharmacol Ther* 103: 147–166.

Higuchi S, Tanaka N, Shioiri Y, Otomo S, Aihara H (1986). Two modes of analgesic action of aspirin, and the site of analgesic action of salicylic acid. *Int J Tissue React* 8: 327–331.

Hilkens CM, Vermeulen H, Joost van Neerven RJ, Snijdewint FGM, Wierenga EA, Kapsenber ML (1995). Differential modulation of T helper type 1 (Th1) and T helper type 2 (Th2) cytokine secretion by prostaglandin E2 critically depends on interleukin-2. *Eur J Immunol* 25: 59–63.

Honda T, Segi-Nishida E, Miyachi Y, Narumiya S (2006). Prostacyclin-IP signaling and prostaglandin E2-EP2/EP4 signaling both mediate joint inflammation in mouse collagen-induced arthritis. *J Exp Med* 203: 325–335.

Hunninghake GW, Monick MM, Liu B, Stinski MF (1989). The promoter-regulatory region of the major immediate-early gene of human cytomegalovirus responds to T-lymphocyte stimulation and contains functional cyclic AMP-response elements. *J Virol* 63: 3026–3033.

Iwanami K, Matsumoto I, Tanaka-Watanabe Y, Mihira M, Ohsugi Y, Mamura M *et al.* (2008). Crucial role of IL-6/IL-17 axis in the induction of arthritis by glucose-6-phosphate isomerase. *Arthritis Rheum* 58: 754–763.

Jones RL, Giembycz MA, Woodward DF (2009). Prostanoid receptor antagonists: development strategies and therapeutic applications. *Brit J Pharm* 158: 104–145.

Joosten LA, Helsen MM, van de Loo FA, van den Berg WB (1996). Anti-cytokine treatment of established type II collagen-induced arthritis in DBA/1 mice. A comparative study using anti-TNF-α, anti-IL-1 α/β, and IL-1Ra. *Arthritis Rheum* 39: 797–809.

Khayrullina T, Yen JH, Jing H, Ganea D (2008). In vitro differentiation of dendritic cells in the presence of prostaglandin E2 alters the IL-12/IL-23 balance and promotes differentiation of Th17 cells. *J Immunol* 181: 721–735.

Kop EN, Adriaansen J, Smeets TJM, Ver voordeldonk M, Tier RA, Hamann J *et al.* (2006). CD97 neutralisation increases resistance to collagen-induced arthritis in mice. *Arthritis Res Ther* 8: R155.

Kuligowska M, Odrowaz-Sypniewska G (2004). Role of interleukin-17 in cartilage and bone destruction in rheumatoid arthritis. *Ortop Traumatol Rehabil* 6: 235–241.

Kunikata T, Yamane H, Segi E, Matsuoka T, Sugimoto Y *et al.* (2005). Suppression of allergic inflammation by the prostaglandin F receptor subtype EP3. *Nature Immunol* 6: 524–531.

Lin CR, Amaya F, Barrett L, Wang H, Takada J, Samad TA *et al.* (2006). Prostaglandin E2 receptor EP4 contributes to inflammatory pain hypersensitivity. *J Pharmacol Exp Ther* 319: 1096–1103.

McCoy JM, Wicks JR, Audoly LP (2002). The role of prostaglandin E_2 receptors in the pathogenesis of rheumatoid arthritis. *J Clin Invest* 110: 651–658.

Matsumoto I, Zhang H, Yasukochi T, Iwanami K, Tanaka Y *et al.* (2008). Therapeutic effects of antibodies to tumor necrosis factor-α, interleukin-6 and cytotoxic T-lymphocyte antigen 4 immunoglobulin in mice with glucose-6-phosphate isomerase induced arthritis. *Arthritis Res Ther* 10: R66.

Murase A, Okumura T, Sakakibara A, Tonai-Kachi H, Nakao K, Takada J (2008). Effect of prostanoid EP_4 antagonist, CJ-042,794, in rat models of pain and inflammation. *Eur J Pharm* 580: 116–121.

Mustelin M, Tasken K (2003). Positive and negative regulation of T cell activation through kinases and phosphatases. *Biochem J* 371: 15–27.

Nakao K, Murase A, Ohshiro H, Okumura T, Taniguchi K, Murata Y *et al.* (2007). CJ-023,423 a novel, potent and selective prostaglandin EP4 receptor antagonist with antihyperalgesic properties. *J Pharmacol Exp Ther* 322: 686–694.

Napolitani G, Acosta-Rodriguez EV, Lanzavecchia A, Sallusto F (2009). Prostaglandin E2 enhances Th17 responses via modulation of IL-17 and IFN-gamma production by memory CD4+ T cells. *Eur J Immunol* 39: 1301–1312.

Ochi T, Ohkubo O, Mutoh S (2003). Role of cyclooxygenase-2, but not cyclooxygenase-1, on type II collagen-induced arthritis in DBA/1J mice. *Biochem Pharmacol* 66: 1055–1060.

Okano M, Sugata Y, Fujiwara T, Matsumoto R, Nishibori M, Shimizu K *et al.* (2006). Prostanoid 2 (EP2)/EP4-mediated suppression of antigen-specific human T cell responses by prostaglandin E2. *Immunol* 118: 343–352.

Regan J (2003). EP2 and EP4 prostanoid receptor signalling. *Life Sci* 74: 143–153.

Schnurr M, Toy T, Shin A, Wagner M, Cebon J, Maraskovsky E (2005). Extracellular nucleotide signaling by P2 receptors inhibits IL-12 and enhances IL-23 expression in human dendritic cells: a novel role for the cAMP pathway. *Blood* 105: 1582–1589.

Schulze-Koops H, Kalden JR (2001). The balance of Th1/Th2 cytokines in rheumatoid arthritis. *Best Pract Res Clin Rheumatol* 15: 677–691.

Sheibanie AF, Tadmori I, Jing H, Vassiliou E, Ganea D (2004). Prostaglandin E2 induces IL-23 production in bone marrow-derived dendritic cells. *FASEB J* 18: 1318–1320.

Sheibanie AF, Khayrullina T, Safadi FF, Ganea D (2007a). Prostaglandin E2 exacerbates collagen-induced arthritis in mice through the inflammatory interleukin-23/interleukin-17 axis. *Arthritis Rheum* 56: 2608–2619.

Sheibanie AF, Yen JH, Khayrullina T, Emig F, Zhang M, Tuma R *et al.* (2007b). The proinflammatory effect of prostaglandin E2 in experimental inflammatory bowel disease is mediated through the IL-23 ->IL-17 axis. *J Immunol* 178: 8138–8147.

Spyvee M, Shaffer CI, Seletsky BM, Schiller S, Liu J, Li X-YL *et al.* (2009). WO 2009/064274 A1.

Takeuchi K, Tanaka A, Kato S, Aihara, Amagase K. (2007). Effect of (S)-4-(1-(5-chloro-2-(4-fluoropheyoxy)benzamido)ethyl) benzoid acid (CJ-42794), a selective antagonist of prostaglandin E receptor subtype 4, on ulcerogenic and healing responses in rat gastrointestinal mucosa. *J Pharmacol Exp Ther* 322: 903–912.

Verri WA Jr, Cunha TM, Parada CA, Poole S, Cunha FQ *et al.* (2006). Hypernociceptive role of cytokines and chemokines: targets for analgesic drug development? *Pharmacol Ther* 112: 116–138.

Williams RO (2004). Collagen-induced arthritis as a model for rheumatoid arthritis. *Methods Mol Med* 98: 207–216.

Williams RO (2006). Pathogenesis and therapy of rheumatoid arthritis. *Ernst Schering Found Symp Proc* 1: 107–130.

Williams RO, Marinova-Mutafchieva L, Feldmann M, Maini RN (2000). Evaluation of TNF-α and IL-1 blockade in collagen-induced arthritis and comparison with combined anti-TNF-α/anti-CD4 therapy. *J Immunol* 165: 7240–7245.

Yao C, Sakata D, Esaki Y, Li Y, Matsuoka T, Kuroiwa K *et al.* (2009). Prostaglandin E(2)-EP4 signaling promotes immune inflammation through Th1 cell differentiation and Th17 cell expansion. *Nat Med* 2009 May 24. [Epub ahead of print].

Supporting Information

Additional Supporting Information may be found in the online version of this article:

Figure S1 Modulation of CMV promoter activity by ER-819762. Our initial drug screen utilized the cytomegalovirus immediate-early (CMV) promoter driving expression of a protein unrelated to the prostanoid receptors in HEK/293 cells. After we observed down-regulation of protein expression by ER-819762, we examined activity of the CMV promoter by stably transfecting a plasmid containing the Renilla luciferase reporter driven by the CMV promoter (pRL-CMV; Promega) into HEK/293 cells. Cells were cultured overnight in DMEM media supplemented with 0.1% fatty-acid free bovine serum albumin (Sigma A0281), and *Renilla* luciferase activity was assayed the next day (Promega Renilla Luciferase assay kit). Addition of 10% fetal bovine serum (FBS) to the cultures up-regulated CMV activity, and this induction was suppressed by 1 $\mu mol \cdot L^{-1}$ ER-819762. Pre-treatment of FBS by incubation with activated charcoal (CSFBS), which removes a variety of lipids, abolished induction of the CMV promoter. Activity could be restored by addition of prostaglandin E_2 (PGE_2) to CS-FBS, and this activity was inhibited by ER-819762. Addition of the cAMP-inducing agent forskolin (FSK) could also induce CMV activity, but this induction was not suppressed by ER-819762. FBS that had been immunodepleted using anti-PGE_2 antibodies (ΔP-FBS: Cayman Chemicals, clone 2B5) was not able to induce CMV activity, indicating that the CMV-inducing activity present in FBS is PGE_2 or a PGE_2-related molecule.

Figure S2 PGE_2 induction of cAMP signalling in HEK/293 cells is mediated by EP_4. HEK/293 cells were stably transfected with a vector containing response elements for the CREB transcription factor driving expression of a secreted alkaline phosphatase reporter (CRE-PLAP). This reporter construct can be up-regulated by stimuli that induce intracellular cAMP, as shown here for forskolin. We also stimulated these cells with PGE_2 ($EP_{1,}$ $_{2,}$ $_{3,}$ and $_4$ agonist), butaprost (EP_2 agonist) or PGE_1-OH (EP_3 and $_4$ agonist). We observed induction of PLAP activity in response to forskolin, PGE_2 or PGE_1-OH, but not to butaprost. ER-819762 could suppress induction by PGE_2 or PGE_1-OH (data not shown). We also saw no induction of CRE-PLAP by up to 100 $nmol \cdot L^{-1}$ sulprostone, an agonist of EP_3 and EP_1 (data not shown). These data indicate that of the four PGE_2 receptors, only EP_4 is able to induce cAMP signalling in HEK/293 cells.

Figure S3 Effect of ER-819762 on Th1 cell differentiation. Naive $CD4^+$ T cells from BALB/c mice were stimulated with α-CD3/α-CD28 under Th1-promoting conditions in the presence or absence of exogenous PGE_2, butaprost, PGE_1-OH plus increasing amount of ER-819762 for 3 days. IFN-γ production (solid bars) was analyzed by ELISA and cell proliferation/viability (open bars) was monitored by AlamarBlue assay.

Figure S4 Effect of anti-PGE_2 antibody on IL-23 mediated Th17 cell expansion. Total $CD4^+$ T cells were stimulated with α-TCRβ/α-CD28 ± 30 $ng \cdot mL^{-1}$ IL-23 in the presence or absence of α-PGE_2 antibody for 5 days. No exogenous PGE_2 was added in these experiments. The number of IL-17 cells was analyzed by IL-17 intracellular staining and showed that treatment with α-PGE_2 antibody results in a striking decrease in the proportion of IL-17-producing cells induced by IL-23.

Figure S5 PGE_2 treatment induces mRNA expression of IL-23R, RORγt and IL-17A during Th17 cell development. Total $CD4^+$ T cells were stimulated with α-TCRβ/α-CD28 ± 30 $ng \cdot mL^{-1}$ IL-23 in the presence or absence of 10 $nmol \cdot L^{-1}$ PGE_2 or 100 $nmol \cdot L^{-1}$ PGE_1-OH (a) or in the presence or absence of 1 $\mu mol \cdot L^{-1}$ ER-819762 or 10 $\mu g \cdot mL^{-1}$ α-PGE_2 Ab (b) for 5 days. Total RNA was isolated and analysed by real-time PCR for the expression of IL-23R, RORγt and IL-17A mRNA.

Please note: Wiley-Blackwell are not responsible for the content or functionality of any supporting materials supplied by the authors. Any queries (other than missing material) should be directed to the corresponding author for the article.

doi:10.1111/j.1741-4520.2010.00270.x

CASE REPORT

Brachmann-de Lange syndrome with congenital diaphragmatic hernia and *NIPBL* gene mutation

Shinichi Hosokawa[1], Nobumasa Takahashi[1], Hiroyuki Kitajima[1], Masahiro Nakayama[2], Kenjirou Kosaki[3], and Nobuhiko Okamoto[4]

Departments of [1]Neonatology, [2]Pathology, and [4]Developmental Pediatrics, Osaka Medical Center and Research Institute for Maternal and Child Health, and [3]Department of Pediatrics, Keio University School of Medicine, Osaka, Japan

ABSTRACT **We report herein a case of Brachmann-de Lange syndrome complicated with congenital diaphragmatic hernia in which a *NIPBL* gene mutation was identified. A female infant born at 37 weeks of gestation died 134 min after delivery, even though endotracheal intubation and resuscitation were performed immediately after the scheduled caesarean operation. We diagnosed the infant with Brachmann-de Lange syndrome from her physical characteristics. An abnormal peak at the 29th exon in the translation area of the *NIPBL* gene was detected using denaturing high-performance liquid chromatography. In addition, a mutation of cytosine to thymine (nonsense mutation) at the 5524th base was identified using the direct sequence method. This variation was likely the cause of the syndrome.**

Key Words: Brachmann-de Lange syndrome, congenital diaphragmatic hernia, denaturing high-performance liquid chromatography, direct sequence method, gene mutation

INTRODUCTION

Brachmann-de Lange syndrome (BDLS) is a multiple congenital anomaly syndrome characterized by growth and mental retardation, variable anomalies of the upper limbs and a peculiar face with hypertrichosis. A pediatrician named de Lange (1933) reported two cases of this disease while working at Amsterdam University in the Netherlands, and termed the disease Cornelia de Lange syndrome. It was subsequently revealed that Brachmann (1916) had reported on a patient exhibiting the same symptoms. As a result of these two reports, the condition is currently known as Brachmann-de Lange syndrome (Opitz 1985).

Brachmann-de Lange syndrome was originally thought to be related to 3q partial trisomic syndrome, as the clinical manifestations of the two diseases are relatively similar. More recently, Krantz *et al.* (2004) and Tonkin *et al.* (2004) reported a variation in the *NIPBL* gene in a BDLS patient, allowing the two diseases to be more easily distinguished.

We report herein a case of BDLS with congenital diaphragmatic hernia caused by a mutation in the *NIPBL* gene that was identified using denaturing high-performance liquid chromatography.

Case report

A 21-year-old woman delivered a female infant at 37 weeks and 2 days of gestation by scheduled caesarean operation due to intrauterine growth retardation and congenital diaphragmatic hernia diagnosed by fetal echography at a gestational age of 30 weeks and 2 days. The infant's birthweight was 1766 g (–2.6 SD) and her Apgar score was 1 at 1 min and 3 at 5 min. When the infant was born, her entire body was pale and she did not demonstrate spontaneous breathing patterns. Endotracheal intubation was immediately performed and artificial ventilation with high frequency oscillation (HFO) and nitric oxide inhalation therapy was initiated. Unfortunately, there was no improvement in her condition, even following the administration of resuscitative medication, including adrenaline and surfactant, and she died 134 min after birth.

We considered that the patient had BDLS due to her characteristic facial features, including synophrys, brachyrrhinia, long philtrum, thin lip, small mandible and short cervix, and the presence of hirsutism and a congenital diaphragmatic hernia. Although her limbs were small and short, and a bilateral single transverse palmar crease was recognized on each hand, the BDLS characteristics of syndactyly and limb reduction defects were not observed (Fig. 1).

At laboratory examination at birth, we identified slight acidosis; however, significant abnormal findings, including anemia and electrolyte imbalance in the cord blood were not observed. The infant's blood gas (venous blood) at 47 min after birth was also recognized as mixed acidosis of pH 6.763, PCO_2 188.0 mmHg, PO_2 3.2 mmHg and BE –16.5 mmol/L. Her hemoglobin was 6.8 g/dL, her C-reactive protein (CRP) was negative and there was no elevation in liver enzyme levels. Hypernatremia was observed in her electrolytes (Table 1). Amniotic fluid chromosomes were of a normal karyotype of 46, XX. X-ray of the entire body revealed a hanging bell-shaped thoracic cage, low pneumatization in the bilateral lungs and a stomach bubble in the middle thorax (Fig. 2).

Pathological autopsy of the infant was undertaken after we obtained informed consent from her parents. The placental weight was 190 g, which was small for the number of gestational weeks (our center average is 514 g), villi were immature and the umbilical cord contained a single umbilical artery. The left diaphragm was almost entirely defective and the liver, stomach, spleen, pancreas, small intestine and large intestine protruded into the intrathoracic area. Marked hypoplasia of the lungs was also recognized with a pulmonary weight ratio of 0.003 (normal is 0.012). In addition, the lungs were histologically immature. Bilateral hydroureter, annular pancreas and atrial septal defect were also observed. We did not examine the brain, as the parents did not consent to craniotomy.

After we obtained written informed consent from the parents for gene diagnosis, we extracted genomic DNA from the patient's blood and amplified the coding region (extending from the 2nd exon to the 47th exon) of the *NIPBL* gene using polymerase chain reaction (PCR). An abnormal peak in exon 29 was detected when analyzed using denaturing high-performance liquid

Correspondence: Shinichi Hosokawa, MD, Murodou-chou 840, Izumi City, Osaka 594-1101, Japan. Email: sinhoso@mac.com

Received February 8, 2009; revised and accepted December 12, 2009.

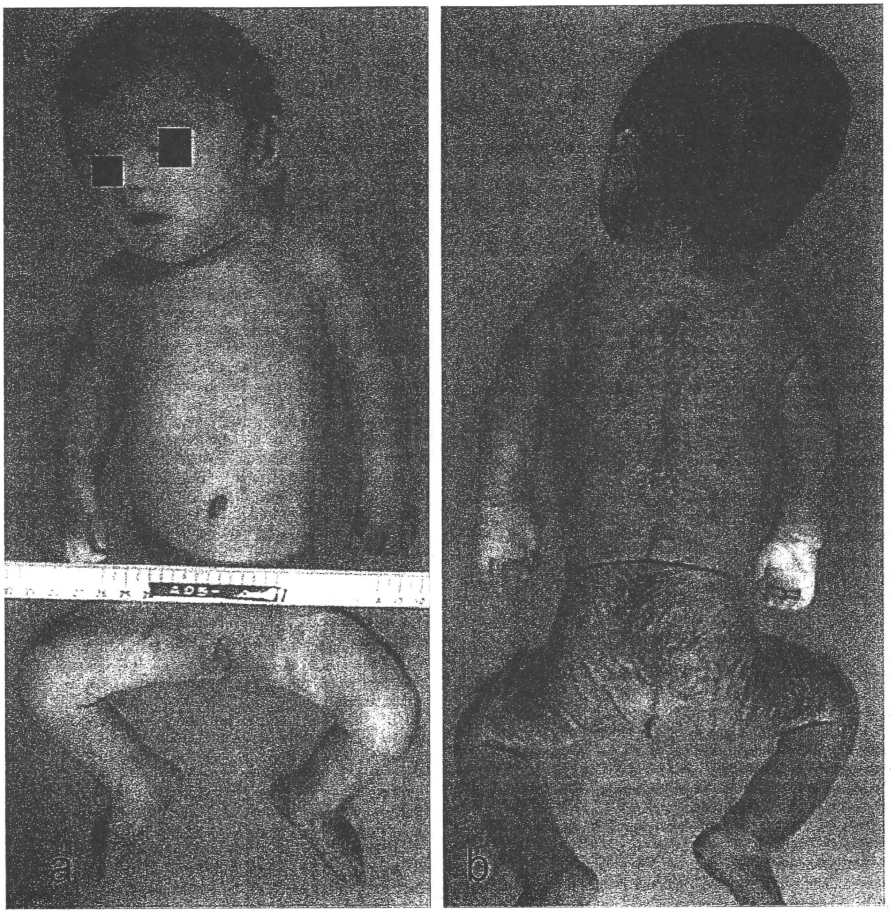

Fig. 1 Photographs highlighting the patient's symptoms (a,b) including hypertrichosis, short extremities, hypoplasia of the nipple and umbilicus, synophrys of the face, short and upturned nose or anteverted nostrils, long philtrum, thin lip, small mandible, short cervix and single bimanual palmar flexion curve without syndactyly or defects of the fingers.

chromatography (Fig. 3). Within the translation area of the *NIPBL* gene, a mutation of cytosine (C) to thymine (T) (nonsense mutation) at the 5524th base was identified using the direct sequence method. This amino acid change formed a stop codon, a result that we hypothesized would influence the complications in this patient.

DISCUSSION

Cornelia de Lange (1933) identified 10 traits, such as mental retardation, low birthweight, dwarfism, microbrachycephaly, heavy eyebrows meeting at the midline, long eyelashes, low-set ears, small hands and feet, proximal placed thumb and syndactyly of the toes in two patients while working at Amsterdam University. Beck (1976) later reported the original diagnostic standards of BDLS (Table 2) and suggested that patients with BDLS could be diagnosed if they exhibited eight of these 10 traits. In the current case, BDLS was not diagnosed in the fetal period, but was diagnosed after birth. The infant demonstrated nine of the traits described by de Lange and five of the traits described in the Beck standards. After confirming our findings with both the de Lange

Table 1 Examination of the umbilical cord and peripheral blood of the present case of Brachmann-de Lange syndrome with congenital diaphragmatic hernia and *NIPBL* gene mutation

	Cord blood	Patient's blood (47 min after birth)
Blood gas analysis		
pH	7.276	6.763
pCO_2	48.9 mmHg	188.0 mmHg
pO_2	20.5 mmHg	3.2 mmHg
Base excess	−4.3 mmol/L	−16.5 mmol/L
Blood cell counts		
White blood count	5900/μL	4900/μL
Platelet count	221 000/μL	93000/μL
Chemistry		
C-reactive protein	<0.05 mg/dL	<0.1 mg/dL
Sodium	140 mmol/L	183 mmol/L
Potassium	4.5 mmol/L	5.3 mmol/L
Calcium	9.5 mg/dL	8.3 mg/dL
Hemoglobin	13.6 g/dL	6.8 g/dL

Table 2 Findings in the present case of Brachmann-de Lange syndrome with congenital diaphragmatic hernia and *NIPBL* gene mutation

	This patient's findings
Cornelia de Lange (1933)	
Mental retardation	?
Low birthweight	+
Dwarfism	?
Microbrachycephaly	+
Heavy eyebrows meeting at the midline	+
Long eyelashes	+
Low ear insertion	−
Small hands and feet	+
Proximally placed thumb	−
Syndactyly of the toes	−
Beck (1976)	
Low hair line on forehead	+
Low hair line on neck	+
Long philtrum	+
Bushy eyebrows	+
Confluent eyebrows	+
Thick eyelashes	+
Antimongoloid eye slanting	−
Anteverted nostrils	+
Crescent-shaped mouth	+
Thin prolabium	+

+, present; ?, not detected due to early death.

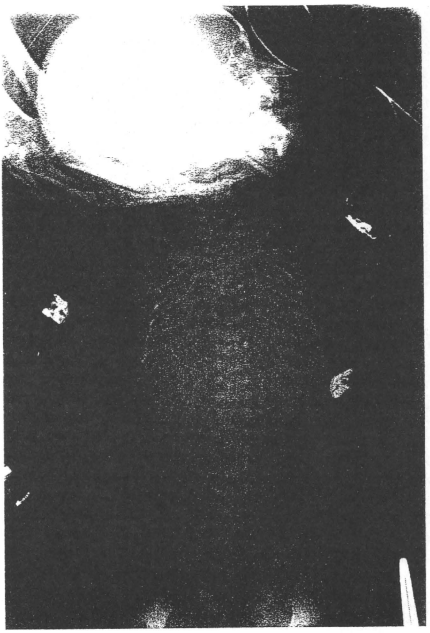

Fig. 2 X-ray of the entire body showing the hanging bell-shaped thoracic cage, low pneumatization in the bilateral lungs and a stomach bubble located in the middle thorax.

and Beck standards, we finally made a diagnosis based on the baby's physical characteristics.

This patient was also diagnosed based on the presence of intrauterine growth retardation and diaphragmatic hernia during the fetal period. Limb shortening was also observed. In the absence of abnormal karyotype or altered bone structures with limb shortening, BDLS is generally considered as a differential diagnosis (Beck and Fenger 1985; Kenneth 1988). Further, the placenta weighed only 190 g, which was low for the gestational period. This finding was consistent with the hypothesis that growth of not only the fetus, but also of the placenta is inadequate in cases of BDLS.

There have been only a few reports of BDLS with congenital diaphragmatic hernia in Japan (Kuroiwa *et al.* 1990; Suzuki *et al.* 1999). A small number of reports (e.g. Cunniff *et al.* (1993), Russel *et al.* (1993) and Marino *et al.* (2002)) have been described in other countries. The reports by these groups suggested that the prognosis was worse when the patient also exhibited congenital diaphragmatic hernia. The precise causes of congenital diaphragmatic hernia remain unknown. BDLS, Fryns syndrome, Goltz syndrome and Smith-Lemli-Opitz syndrome are all associated with congenital diaphragmatic hernia (Tibboel and Gaag 1996; Bianch *et al.* 2000). Recently, gene analysis of these various multiple malformation syndromes has been undertaken (Holder *et al.* 2007). Further gene

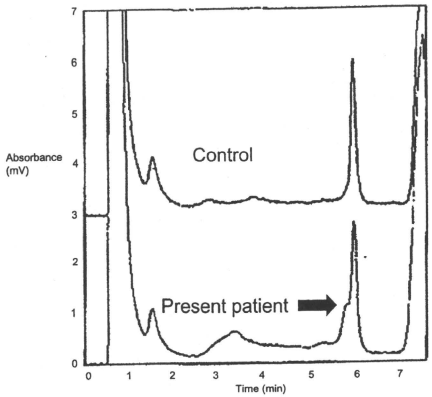

Fig. 3 Denaturing high-performance liquid chromatography of the 29th exon of the *NIPBL* gene (upper panel: control, lower panel: patient). Arrow shows the abnormal peak in the translation area (29th exon) of the *NIPBL* gene.

analyses in the various multiple malformation syndromes specifically associated with congenital diaphragmatic hernia are likely to shed light on which anomalies lead to diaphragmatic hernia.

In the present case, a mutation of C to T (nonsense mutation) at the 5524th base in the translation area of the *NIPBL* gene was identified. As a result, we concluded that this variation was likely to be the cause of the BDLS with diaphragmatic hernia. The *NIPBL* gene is located at 5p13.1 and contains 47 exons, and its transcription is thought to be related to Notch signal transmission. There have been many confirmed gene mutations, including deletion and insertion mutations, that are associated with BDLS (Gillis *et al.* 2004; Bhuiyan *et al.* 2006; Schoumans *et al.* 2007). Further, Musio *et al.* (2006) and Deardorff *et al.* (2007) have presented reports relating BDLS to both *SMC1* and *SMC3* gene mutations.

DNA analysis is important for confirming BDLS diagnosis. Analysis of gene mutations in genes such as *NIPBL* also represents a useful diagnostic method. With the accumulation of cases such as ours, further description of this disease will be possible.

REFERENCES

Beck B (1976) Epidemiology of Cornelia de Lange's syndrome. *Acta Pediatr Scand* **65**: 631–638.

Beck B, Fenger K (1985) Mortality, pathological findings and causes of death in the de Lange syndrome. *Acta Paediatr Sca* **74**: 765–769.

Bhuiyan ZA, Klein M, Hammond P *et al.* (2006) Genotype-phenotype correlations of 39 patients with Cornelia de Lange syndrome: the Dutch experience. *J Med Genet* **43**: 568–575.

Bianch DW, Crombleholme T, D'Alton ME (2000) *Fetology*, 1st edn. McGraw-Hill, New York.

Brachmann W (1916) Ein fall von symmetrischer monodaktylie durch Ulnadefekt, mit symmetrischer flughautbildung in den ellenbeugen, sowie anderen abnormitaten (zwerghaftogkeit, halsrippen, behaarung). *Jerb Kinder Phys Erzie* **84**: 225–235 (in German.)

Cunniff C, Curry CJ, Carey JC *et al.* (1993) Congenital diaphragmatic hernia in the Brachmann-de Lange syndrome. *Am J Med Genet* **47**: 1018–1021.

de Lange C (1933) Sur un type nouveau de degenerescence (typus Amstelodemensis). *Arch Med Enfants* **36**: 713–719. (in French.).

Deardorff MA, Kaur M, Yaeger D *et al.* (2007) Mutations in cohesin complex members SMC3 and SMC1A cause a mild variant of Cornelia de Lange syndrome with predominant mental retardation. *Am J Hum Genet* **80**: 485–494.

Gillis LA, McCallum J, Kaur M *et al.* (2004) NIPBL mutation analysis in 120 individuals with Cornelia de Lange syndrome and evaluation of genotype-phenotype correlations. *Am J Hum Genet* **75**: 610–623.

Holder AM, Klaassens M, Tibboel D *et al.* (2007) Genetic factors in congenital diaphragmatic hernia. *Am J Genet* **80**: 825–845.

Kenneth LJ (1988) *Smith's Recognizable Patterns of Human Malformation*, 6th edn. Elsevier Saunders, Philadelphia.

Krantz ID, McCallum J, DeScipio C *et al.* (2004) Cornelia de Lange syndrome is caused by mutations in NIPBL, the human homolog of drosophila melanogaster Nipped-B. *Nature Genet* **36**: 631–635.

Kuroiwa M, Matsuyama S, Suzuki N *et al.* (1990) [Cornelia de Lange syndrome with the right Bochdalek hernia: A case report with special reference to associated gastroesophageal disorders.]. *Nippon Shounigeka Gakkai Zasshi* **26**: 974–980 (In Japanese.)

Marino T, Wheeler PG, Simpson LL *et al.* (2002) Fetal diaphragmatic hernia and upper limb anomalies suggest Brachmann-de Lange syndrome. *Prenat Diagn* **22**: 144–147.

Musio A, Selicorni A, Focarelli ML *et al.* (2006) X-linked Cornelia de Lange syndrome owing to SMC1L1 mutations. *Nat Genet* **38**: 528–530.

Opitz JM (1985) Editorial comment: the Brachmann de Lange syndrome. *Am J Med Genet* **22**: 89–102.

Russel DJ, Nelson BI, Nadya JK *et al.* (1993) Prenatal diagnosis of congenital diaphragmatic hernia not amenable to prenatal or neonatal repair: Brachmann-de Lange syndrome. *Am J Med Genet* **47**: 1022–1023.

Schoumans J, Wincent J, Barbaro M *et al.* (2007) Comprehensive mutational analysis of a cohort of Swedish Cornelia de Lange syndrome patients. *Eur J Hum Genet* **15**: 143–149.

Suzuki S, Mukai K, Takei Y *et al.* (1999) [A autopsy report of Cornelia de Lange syndrome.]. *Shounika Rinshou* **52**: 1967–1972 (In Japanese.)

Tibboel D, Gaag AVD (1996) Etiological genetic factors in congenital diaphragmatic hernia. *Clin Perinatol* **23**: 689–699.

Tonkin ET, Wang TJ, Lisgo S *et al.* (2004) NIPBL, encoding a homolog of fungal Scc2-type sister chromatid cohesion proteins and fly Nipped-B, is mutated in Cornelia de Lange syndrome. *Nature Genet* **36**: 636–641.

0031-3998/10/6702-0166
PEDIATRIC RESEARCH

Vol. 67, No. 2, 2010
Printed in U.S.A.

Placental Features of Chorioamnionitis Colonized With *Ureaplasma* Species in Preterm Delivery

FUMIHIKO NAMBA, TAEKO HASEGAWA, MASAHIRO NAKAYAMA, TAKURO HAMANAKA, TATSUYUKI YAMASHITA, KUMIKO NAKAHIRA, AKIHITO KIMOTO, MASATOSHI NOZAKI, MASAHIRO NISHIHARA, KAZUYA MIMURA, MINORU YAMADA, HIROYUKI KITAJIMA, NORIYUKI SUEHARA, AND ITARU YANAGIHARA

Departments of Developmental Medicine [F.N., T.H., K.N., M.N., M.N., K.M., M.Y., I.Y.], Pathology and Laboratory Medicine [M.N., A.K.], Obstetrics [T.H., N.S.], and Neonatology [H.K.], Osaka Medical Center and Research Institute for Maternal and Child Health, Izumi, Osaka 594-1101, Japan; Department of Biochemistry [T.Y.], Kochi University Medical School, Nankoku, Kochi 783-8505, Japan

ABSTRACT: *Ureaplasma* spp. is detected in the urogenital tract, including the vagina, cervix, chorioamnion, and placenta. Their colonization is associated with histologic chorioamnionitis (CAM), often observed in placentas from preterm delivery. We isolated *Ureaplasma* spp. from 63 preterm placentas among 151 specimens, which were delivered at <32 wk of gestation. Of the 63 placentas, 52 (83%) revealed CAM in cultures positive for *Ureaplasma* spp., however, CAM was observed only in 30% (26/88) of cultures negative for *Ureaplasma* spp. ($p < 0.01$). Colonization by *Ureaplasma* spp. was an independent risk factor for CAM (OR, 11.27; 95% CI, 5.09–24.98). Characteristic neutrophil infiltration was observed in the amnion and subchorion (bistratified pattern) in cultures positive for *Ureaplasma* spp. FISH analysis of CAM placenta with male infant pregnancy indicated that bistratified infiltrated neutrophils showed the XX karyotype and umbilical vein infiltrated neutrophils showed XY karyotype. The distribution of sulfoglycolipid, the receptor of *Ureaplasma* spp., was mainly detected in the amnion. Ureaplasmal urease D protein and *ureB* gene were both detected in the amnion, indicating direct colonization by *Ureaplasma* spp. **(*Pediatr Res* 67: 166–172, 2010)**

Ureaplasma spp. is the smallest self-replicating organism, both in genome size and in cellular dimensions. It lacks cell walls and exists in association with eukaryotic cells, mainly colonizing mucosal surfaces of the respiratory and urogenital tracts (1). *Ureaplasma* spp. is a common inhabitant of the lower genital tract and isolated from 40 to 80% women of child-bearing age (2). However, once *Ureaplasma* spp. spreads from the lower genital tract into the body, this microorganism exerts widespread pathogenic effects, such as chorioamnionitis (CAM), urinary tract infections, preterm labor, and spontaneous abortion. On the other hand, *Ureaplasma* spp. infection is also reported as a risk factor for lethal pneumonia, chronic lung disease, and meningitis of fetuses and neonates (3).

CAM is a placental finding associated with premature rupture of membranes (PROM) and preterm birth, which are the most important causes of perinatal morbidity and mortality (4,5). Previous studies showed that CAM was positively related to the isolation of *Ureaplasma* spp (6,7). Although many researchers reported the detection of *Ureaplasma* spp. from specimens of vagina, cervix, chorioamnion, and placenta using culture or PCR methods (8–12), the precise pathologic findings of CAM with *Ureaplasma* spp. remain unclear.

A variety of infectious microorganisms use specific host cell surface molecules as receptors. Such receptors provide a mechanism for intimate interaction with the host cell membrane and in some cases may facilitate the subsequent entry of the organism into the cell (13). *Ureaplasma* spp. and *Mycoplasma hominis* were shown to specifically recognize host cell surface glycolipids (sulfogalactoglycerolipid and the sphingolipid counterpart, sulfogalactosyl ceramide), which have been implicated in sperm-egg interactions (14). This glycolipid receptor binding may relate to the reproductive pathogenesis of these organisms. Furthermore, there are no previous reports about the specific receptor of *Ureaplasma* spp. and its distribution in the placenta.

This study was conducted to confirm the prevalence of placental *Ureaplasma* spp. in preterm delivery, and whether there is an association between *Ureaplasma* spp. and CAM. Moreover, we identified placental features that might be characteristic of ureaplasmal infection.

METHODS

Subjects and placental examination. All clinical specimens were obtained after informed consent approved by the Ethics Committee of Osaka Medical Center and Research Institute for Maternal and Child Health. In this study from January to December 2007, pathologic examinations of 151 placentas, including 67 cesarean deliveries, delivered at <32 wk of gestation were performed. As a control, 41 term placentas [mean gestational age, 39.6 wk (SD 1.1); mean birth weight, 3009 g (SD 425)], including 11 cesarean deliveries (27%), four PROM (10%), and two intrauterine growth retardation (5%), were also examined. The pathologists who examined the placentas were blinded to the results of *Ureaplasma* spp. culture. Placentas were examined according to the method of Fox and Sebire (15). The histologic criterion used for CAM was the presence of accumulated leukocytes extending through the fetal membranes using Blanc's classification (16). Umbilical vasculitis was defined as migration of fetal inflammatory cells into or through the media of the umbilical arteries or veins. The criterion used for subacute necrotizing funisitis was a typical deposition of calcification around the vessels in the umbilical cord.

Received May 21, 2009; accepted September 27, 2009.

Correspondence: Itaru Yanagihara, M.D., Ph.D., Department of Developmental Medicine, Osaka Medical Center and Research Institute for Maternal and Child Health, 840 Murodo-cho, Izumi, Osaka 594-1101, Japan; e-mail: itaruy@mch.pref.osaka.jp

Supported by grants-in-aid from the Ministry of Health, Labor and Welfare, Japan; Ministry of Education, Culture, Sports, Science and Technology (MEXT), Japan; Research on Child Health and Development, Japan; and The Foundation for Mother and Child Well-being, Osaka, Japan.

F.N. and T.H. contributed equally to this study.

Abbreviations: CAM, chorioamnionitis; **GBS,** group B *Streptococcus*; **PROM,** premature rupture of membranes; **TLR,** toll-like receptor

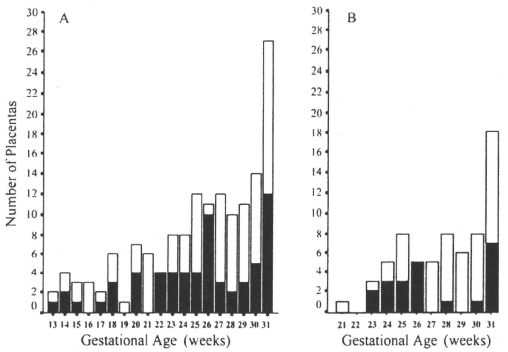

Figure 1. Isolation of *Ureaplasma* spp. from preterm placenta. Forty-two percent (63/151) of preterm placentas (<32 wk) were culture positive for *Ureaplasma* spp. (*A*), and 33% (22/67) in preterm cesarean delivery, (*B*) black bars, culture positive for *Ureaplasma* spp.; white bars, culture negative for *Ureaplasma* spp.

Culture for the detection of* Ureaplasma *spp. A microbiologist who was blinded to all clinical details of the patients prepared cultures for the detection of *Ureaplasma* spp.; species identification and subtyping of *Ureaplasma* spp. were also developed. The placental swabs were collected from the fetal side of the placentas. These were suspended in UMCHs medium: *Mycoplasma* broth base (Becton, Dickinson and Co., Baltimore, MD) 1.47% (wt/vol), yeast extract (Becton, Dickinson and Co.) 2.5% (wt/vol), horse serum (Biowhittaker, Walkersville, MD) 20% (vol/vol), supplement VX (Becton, Dickinson and Co.) 1.0% (vol/vol), urea 0.04% (wt/vol), phenol red 0.001% (wt/vol), L-cysteine hydrochloride 0.01% (wt/vol), and penicillin G 1000 U/mL. After incubation at 35°C for up to 72 h, the color of the medium changed from yellow to red due to hydrolysis of urea, and these color changes were regarded as indicating positivity for *Ureaplasma* spp. We identified *Ureaplasma* spp. by colony formation and subsequent PCR-based assays using modified Kong's method (17).

Immunohistochemistry. Paraffin-embedded sections were deparaffinized and rehydrated. The sections were incubated with rabbit anti-human myeloperoxidase polyclonal antibody (1:300; Dako, Tokyo, Japan), mouse anti-human cluster of differentiation (CD) 45 MAb (1:1; Thermo/Shandon Immunon, Pittsburgh, PA), mouse anti-human CD68 MAb (1:50; Dako), chicken anti-*Ureaplasma urealyticum* UreD polyclonal antibody (1:100; Abcam, Cambridge, MA), and mouse anti-sulfoglycolipid MAb (1:5) (18). Immunoreactivity was detected using the Envision Kit (Dako) with horseradish peroxidase-conjugated anti-chicken IgG antibody (1:200; Bethyl Laboratories, Montgomery, TX). Sections were counterstained with Mayer's hematoxylin (Muto Pure Chemicals, Tokyo, Japan).

FISH analysis. X/Y FISH was performed using the CEP X/Y DNA Probe Kit (Vysis, Downers Grove, IL) according to the manufacturer's instructions. Included in this kit are probes for Xp11.1-q11.1 of chromosome X (labeled with Spectrum Red) and for Yq12 of chromosome Y (labeled with Spectrum Green). Fluorescence microscope (Olympus IX71 microscope; Olympus, Tokyo, Japan) integrated with a digitized CCD camera (Nikon Digital Sight DS-5Mc, Nikon Instech, Kanagawa, Japan) and imaging software (Nikon ACT-2U Nikon) were used to investigate and analyze the FISH results with DAPI II counterstain.

PCR for the detection of* Ureaplasma *urease structural gene. DNA was extracted from paraffin-embedded placental sections using DNA Isolator PS-Rapid Reagent (Wako Pure Chemical Industries, Osaka, Japan) according to the manufacturer's instructions. The DNA solution was used for subsequent PCRs. The PCR primers used were as follows: *Glut1*, sense (5′-TGCAAGGGGAAAGGAAAAGG-3′) and antisense (5′-GAAGAGAAACTCTGCCCTGC-3′) of the human facilitative glucose transporter genes; and *ureB*, sense (5′-CCAGGTAA ATTAGTACCAGG-3′) and antisense (5′-CCTGATGGAATATCGAAACG-3′) of the *Ureaplasma* urease structural genes. Twenty-five micro liters of *GoTaq* Green Master Mix (Promega, Madison, WI), 1 μL sample, and 14 μL water were added to each reaction. A thermal cycler was used to process samples through 35 cycles at 95°C for 30 s, 64°C for 30 s, and 68°C for 30 s for *Glut1* and through 35 cycles at 95°C for 30 s, 45°C for 30 s, and 68°C for 30 s for *ureB*.

Statistical analysis. All statistical analyses were performed using SPSS 11.0 for Windows (SPSS, Chicago, IL). The χ^2 test or Fisher's exact test was used to compare the incidence of each placental feature between cases culture positive and negative for *Ureaplasma* spp. Logistic regression models were used to examine the association between culture positivity for *Ureaplasma* spp. and the severity of CAM. The Mann-Whitney *U* test or unpaired *t* test was used to compare continuous variables. A difference was considered significant when the *p* value was <0.05. Logistic regression analysis, adjusting for the potential confounding clinical factors associated with CAM, were conducted to evaluate the independent association of *Ureaplasma* spp. colonization with CAM. The strength of association in these models is reported as the adjusted OR with the 95% CI.

Table 1. *Maternal characteristics associated with* Ureaplasma *spp. colonization*

	Ureaplasma spp. (+) (*n* = 63)	*Ureaplasma* spp. (−) (*n* = 88)	*p*
Gestational age (wk), median (range)	26.4 (13.0–31.9)	27.5 (13.0–31.9)	NS
Birth weight (g), median (range)	742 (0–1878)	753 (0–2280)	NS
Multiple pregnancy	9 (14%)	24 (27%)	NS
Placenta previa	0 (0%)	2 (2%)	
Abruptio placentae	6 (10%)	5 (6%)	NS
Preeclampsia	3 (5%)	15 (17%)	<0.05
Oligohydramnios	19 (30%)	23 (26%)	NS
Polyhydramnios	1 (2%)	5 (6%)	NS
PROM	28 (44%)	14 (16%)	<0.01
Cesarean section	22 (35%)	45 (51%)	<0.05
Culture positive for other microorganism	8 (13%)	5 (6%)	NS

RESULTS

Incidence of* Ureaplasma *spp. colonization in preterm placentas. Among 151 placentas delivered at <32 wk of gestation, 42% (63/151) were culture positive for *Ureaplasma* spp. Figure 1*A* shows the incidence of *Ureaplasma* spp. colonization in preterm placentas according to gestational age. Forty-nine percent (38/77) of placentas delivered during the second trimester (at 13–26 wk) and 34% (25/74) delivered during the early third trimester (at 27–31 wk) were colonized with *Ureaplasma* spp. The incidence of *Ureaplasma* spp. colonization during the second trimester was higher than that during the early third trimester, but the difference was not statistically significant (49% *versus* 34%; $p = 0.05$). The incidence of *Ureaplasma* spp. colonization in term placentas was 24% (10/41); this was significantly lower than that in

Table 2. *Other microorganisms detected in placental cultures*

Culture for *Ureaplasma* spp.	Placenta no.	Other microorganism
Positive (n = 8)	1	*Escherichia coli*
	2	*Pseudomonas fluorescens*
		Enterobacter cloacae
	3	*Candida glabrata*
	4	*Streptococcus mitis*
		Escherichia coli
	5	*Clostridium* spp.
	6	*Gardnerella vaginalis*
	7	*Pseudomonas fluorescens*
	8	*Chrvseobacterium indologenes*
Negative (n = 5)	9	Group B *Streptococcus*
	10	Group B *Streptococcus*
	11	*Escherichia coli*
		Prevotella bivia
	12	Group B *Streptococcus*
	13	Group B *Streptococcus*

Table 3. *Pathological features of placentas with and without* Ureaplasma *colonization*

	Ureaplasma spp. (+) (n = 63) (%)	*Ureaplasma* spp. (−) (n = 88) (%)	p
Gross findings			
Retroplacental hematoma	7 (11)	11 (13)	NS
Thrombosis	4 (6)	4 (5)	NS
Infarction	3 (5)	7 (8)	NS
Fibrin deposition	3 (5)	15 (17)	NS
Histopathological findings			
CAM	52 (83)	26 (30)	<0.01
CAM with umbilical cord inflammation	29 (46)	6 (07)	<0.01
Meconium staining	0 (0)	1 (1)	
Hemosiderin pigmentation	5 (8)	4 (5)	NS
Subacute necrotizing funisitis	4 (6)	0 (0)	
Villitis	0 (0)	3 (3)	
Fibrin deposition	0 (0)	1 (1)	
Syncytial knot	2 (3)	6 (7)	NS

preterm placentas (24% *versus* 42%; $p < 0.05$). On the contrary, 33% (22/67) of preterm cesarean delivery placentas (at 21–31 wk) were culture positive for *Ureaplasma* spp. (Fig. 1*B*).

Maternal characteristics associated with* Ureaplasma *spp. colonization. Maternal characteristics of the *Ureaplasma*-positive and -negative groups are shown in Table 1. The incidence of PROM in the *Ureaplasma*-positive group was significantly higher than that in the negative group (44% *versus* 16%; $p < 0.01$). The incidences of pre-eclampsia and cesarean section in the *Ureaplasma*-positive group were lower than those in the negative group (5% *versus* 17%, $p < 0.05$; 35% *versus* 51%, $p < 0.05$, respectively). There were no significant differences between these two groups in other maternal characteristics. Other microorganisms cultured from placentas are listed in Table 2. Among 151 placentas, only 13 (9%) were culture positive for other microorganisms, the most frequent of which were group B *Streptococcus* (GBS) and *Escherichia coli*.

Pathologic features of placentas in* Ureaplasma*-positive group. Placental findings in the *Ureaplasma*-positive and -negative groups are presented in Table 3. Placentas of the *Ureaplasma*-positive group showed a significantly higher frequency of CAM compared with the negative group (83% *versus* 30%; $p < 0.01$). CAM with umbilical cord inflammation was also more frequent in the *Ureaplasma*-positive group than in the negative group (46% *versus* 7%; $p < 0.01$). No differences were found in the percentages of any other findings between these two groups.

Table 4. *Risk factors for CAM*

	Univariate		Multivariate	
	OR	95% CI	OR	95% CI
Culture positive for *Ureaplasma* spp.	11.27	5.09–24.98	8.60	3.72–19.89
Multiple pregnancy	0.45	0.20–01.00	0.63	0.24–01.62
PROM	7.67	3.13–18.84	5.36	1.98–14.52
Culture positive for other microorganism	3.43	0.91–13.01	2.90	0.58–14.52

Table 5. *Pathological features of CAM placentas with and without* Ureaplasma *colonization*

	Ureaplasma spp. (+) (n = 52) (%)	*Ureaplasma* spp. (−) (n = 26) (%)	p
Severity			
Blanc I	3 (6)	9 (35)	—
Blanc II	14 (27)	8 (31)	<0.05
Blanc III	35 (67)	9 (35)	<0.01
Distribution			
Amniotic bistratified pattern	18 (35)	2 (8)	<0.05
Umbilical cord inflammation			
Umbilical vasculitis	29 (56)	6 (23)	<0.05
Subacute necrotizing funisitis	4 (8)	0 (0)	

Association of* Ureaplasma *spp. colonization with CAM. Table 4 displays ORs for the strength of association between histologic CAM and risk factors for the development of CAM. Culture positivity for *Ureaplasma* spp. and PROM were significantly associated with CAM (OR, 11.27; 95% CI, 5.09–24.98; and OR, 7.67; 95% CI, 3.13–18.84, respectively). The associations between culture positivity for *Ureaplasma* spp. and CAM and between PROM and CAM remained significant after adjustment for confounding factors in logistic regression analyses (OR, 8.60; 95% CI, 3.72–19.89; and OR, 5.36; 95% CI, 1.98–14.52, respectively).

Characteristics of CAM placentas colonized with* Ureaplasma *spp. To explore the characteristics of preterm CAM placentas colonized with *Ureaplasma* spp., we compared 52 CAM placentas in the *Ureaplasma*-positive group with 26 CAM placentas in the negative group (Table 5). Logistic regression models using Blanc I CAM as the reference showed that culture positivity for *Ureaplasma* spp. was associated with severe CAM (Blanc II and III).

Moreover, we found a characteristic pathologic finding named the "amniotic bistratified pattern," in which a stratified leukocyte infiltration in the amnion and subchorion was accompanied by necrosis of the amniotic epithelium (Fig. 2*A*), in contrast to GBS positive (control) placenta (Fig. 2*B*). This pattern was significantly more frequent in the *Ureaplasma*-positive group than in the negative group (35% *versus* 8%; $p < 0.05$). It counted 51% (18/35) of Blanc III CAM in the *Ureaplasma*-positive group. In all 20 placentas that showed